Targeting bladder urothelial carcinoma with pHLIP-ICG and inhibition of urothelial cancer cell proliferation by pHLIP-amanitin

Anna Moshnikova[1‡], Borivoj Golijanin[2,3‡], Ali Amin[2],
Joshua Doyle[1†], Ohad Kott[3], Boris Gershman[3†],
Michael DuPont[1], Yujing Li[4], Xiongbin Lu[4,5],
Donald M. Engelman[6], Oleg A. Andreev[1],
Yana K. Reshetnyak[1*] and Dragan Golijanin[3*]

[1]Physics Department, University of Rhode Island, Kingston, RI, United States, [2]Department of Pathology and Laboratory Medicine, The Warren Alpert Medical School of Brown University, The Miriam Hospital, Providence, RI, United States, [3]Division of Urology, Department of Surgery, Brown University, The Miriam Hospital, Providence, RI, United States, [4]Department of Medical and Molecular Genetics, Indiana University School of Medicine, Indianapolis, IN, United States, [5]Melvin & Bren Comprehensive Cancer Center, Indiana University School of Medicine, Indianapolis, IN, United States, [6]Department of Molecular Biophysics and Biochemistry, Yale, New Haven, CT, United States

Acidity is a useful biomarker for the targeting of metabolically active cells in tumors. pH Low Insertion Peptides (pHLIPs) sense the pH at the surfaces of tumor cells and can facilitate intracellular delivery of cell-permeable and cell-impermeable cargo molecules. In this study we have shown the targeting of malignant lesions in human bladders by fluorescent pHLIP agents, intracellular delivery of amanitin toxin by pHLIP for the inhibition of urothelial cancer cell proliferation, and enhanced potency of pHLIP-amanitin for cancer cells with 17p loss, a mutation frequently present in urothelial cancers. Twenty-eight *ex-vivo* bladder specimens, from patients undergoing robotic assisted laparoscopic radical cystectomy for bladder cancer, were treated *via* intravesical incubation for 15-60 minutes with pHLIP conjugated to indocyanine green (ICG) or IR-800 near infrared fluorescent (NIRF) dyes at concentrations of 4-8 µM. White light cystoscopy identified 47/58 (81%) and NIRF pHLIP cystoscopy identified 57/58 (98.3%) of malignant lesions of different subtypes and stages selected for histopathological processing. pHLIP NIRF imaging improved diagnosis by 17.3% ($p < 0.05$). All carcinoma-*in-situ* cases missed by white light cystoscopy were targeted by pHLIP agents and were diagnosed by NIRF imaging. We also investigated the interactions of pHLIP-amanitin with urothelial cancer cells of different grades. pHLIP-amanitin produced concentration- and pH-dependent inhibition of the proliferation of urothelial cancer cells treated for 2 hrs at concentrations up to 4 µM. A 3-4x enhanced cytotoxicity of pHLIP-amanitin was observed for cells with a 17p loss after 2 hrs of treatment at pH6. Potentially, pHLIP technology may improve the management of urothelial cancers, including imaging of malignant lesions

using pHLIP-ICG for diagnosis and surgery, and the use of pHLIP-amanitin for treatment of superficial bladder cancers *via* intravesical instillation.
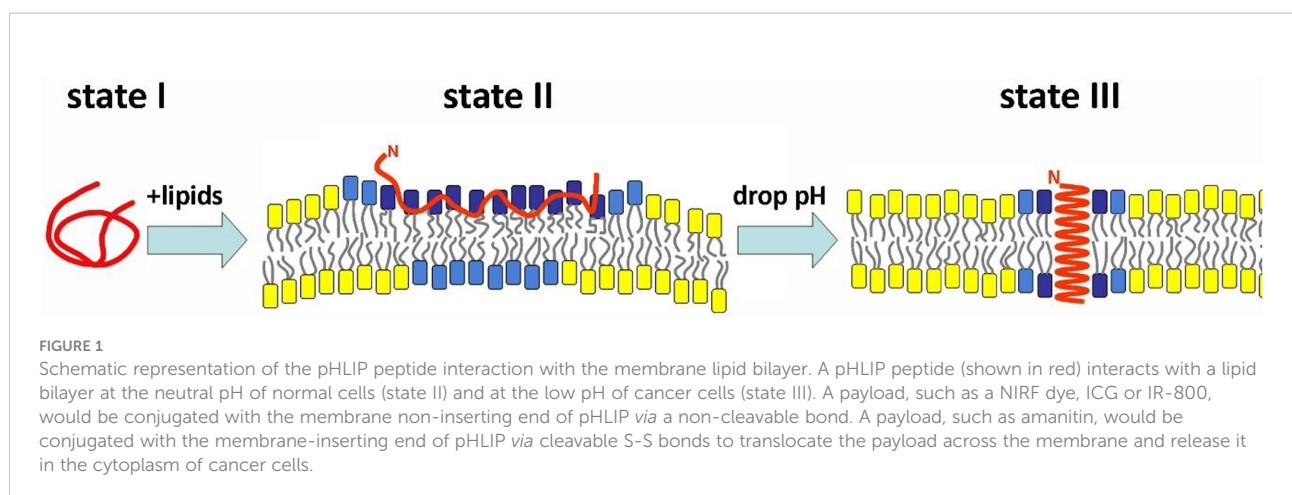
Introduction

Bladder cancer (BC) is the sixth most common cancer worldwide (1). About 75% of all newly diagnosed cases are non-muscle invasive BC (NMIBC) (2). The recurrence rate of NMIBC varies from 30 to 80%, and about 10 to 20% of the recurrent cases progress to muscle-invasive BC (MIBC) within 2–5 years. The medical need to identify and treat NMIBC is high and, if successful, new treatments could reduce mortality and morbidity in patients with BC.

Active efforts to identify diagnostic molecular markers in blood or tissue samples are under development (3, 4), but treatment improvements to eradicate urothelial cancer lesions are needed. Primary treatment options include surgical Trans-Urethral Resection of Bladder Tumors (TURBTs) combined with pre- and/or post-operative intravesical immuno and chemotherapy. Recent statical analysis indicates that Bacillus Calmette–Guérin (BCG) instillation immuno-therapy does not provide long-term benefits over chemotherapy in intermediate-risk NMIBC, while chemotherapy with maintenance reduces the recurrence rate (5). The effectiveness of the most common intravesical chemotherapies, including mitomycin C and gemcitabine, is limited (6). The major issues are i) a lack of specific targeting of cancer cells; ii) limited penetration into the tumor mass; and iii) rapid clearance of small molecule

chemotherapeutics by capillaries, preventing them from acting in the bladder and leading to systemic absorption associated with adverse effects. Novel approaches for targeted delivery of both imaging and therapeutic agents for better visualization of cancer lesions during TURB and improved chemotherapy are needed.

We have explored the use of a pH-Low Insertion Peptide (pHLIP) as a tumor targeting peptide, which senses and targets the low pH at the surfaces of cancer cells (7, 8). Since pHLIP is a moderately hydrophobic peptide, it is reversibly adsorbed by cellular membranes at normal and high pHs (state II, Figure 1). At the moderately low local pH (pH 6.0-6.5) found at the surfaces of cancer cells, pHLIP peptides insert across the cell membrane to form a stable transmembrane helix (state III, Figure 1) (9–11). A variety of imaging and therapeutic agents have been successfully delivered to tumors by pHLIP peptides. The molecular mechanism of action of the acidity targeting by peptides of the pHLIP family has been rigorously investigated in many publications (see review (8) and references within). Imaging of malignant lesions in human bladders and upper urinary tracts has been shown using a near infrared fluorescent (NIRF) dye, ICG (indocyanine green), linked to pHLIP (pHLIP-ICG) (12, 13). When a cargo molecule is attached to the peptide's membrane-inserting end *via* a cleavable S-S link, which is unstable in the reducing environment of the

FIGURE 1
Schematic representation of the pHLIP peptide interaction with the membrane lipid bilayer. A pHLIP peptide (shown in red) interacts with a lipid bilayer at the neutral pH of normal cells (state II) and at the low pH of cancer cells (state III). A payload, such as a NIRF dye, ICG or IR-800, would be conjugated with the membrane non-inserting end of pHLIP *via* a non-cleavable bond. A payload, such as amanitin, would be conjugated with the membrane-inserting end of pHLIP *via* cleavable S-S bonds to translocate the payload across the membrane and release it in the cytoplasm of cancer cells.

cytoplasm, pHLIP peptides can translocate the cargo across the membrane and release it into the cell. We have previously reported the pH-dependent intracellular delivery of alpha-amanitin, phalloidin and phallacidin, which are polar, cell-impermeable deadly toxins using linear and cyclic versions of pHLIPs (14–18).

The goal of our study is two-fold: i) to investigate the specificity and sensitivity of fluorescent pHLIP-ICG for the visualization of cancer lesions in human bladder specimens to potentially improve TURBT outcomes, and ii) to assess pHLIP-amanitin as a toxic agent against urothelial tumor cells to pave the way for targeted chemotherapeutic treatments applied *via* intravesical instillation.

Methods

NIRF imaging on human bladders

We studied bladder lesion targeting by fluorescent pHLIP agents (pHLIP-ICG and pHLIP-IR800) in 28 patients undergoing radical cystectomy for non-metastatic urothelial carcinoma of the bladder at The Miriam Hospital. Excised bladder specimens were irrigated and incubated *ex-vivo* with pHLIP-ICG or pHLIP-IR800 followed by washing. The bladders were opened using a "Y" incision on the anterior wall, followed by careful examination for macroscopic lesions using white light (WL) and NIRF imaging with either a DaVinci Si Surgical System Firefly or a Stryker 1588 AIM imaging system. Randomized control sections were selected from regions with no pHLIP signal and where no lesions were found by WL examination. In all cases, macroscopic lesions found under either WL or NIRF imaging were labeled and thoroughly sampled for pathological analysis, which was performed according to the standard institutional grossing procedure with emphasis on the marked areas of the bladder. Obtained NIRF images were processed using software developed in MATLAB. Diagnostic accuracy was evaluated as sensitivity and specificity compared across WL and NIRF imaging using McNemar's test.

Proliferation of cancer cells treated with pHLIP-amanitin

The cytotoxic *ex-vivo* effect of increasing amounts of pHLIP-amanitin, pHLIP or amanitin was evaluated at various pHs and times of treatment of urothelial (UMUC3, SW780, RT4 - grade 1; 5637 - grade 2; J82, T24, HT-1376 - grade 3; TCCSUP, HT-1197 - grade 4 (19–27)) and breast MDA-MB-231 WT (POLR2A+/+) and isogenic (POLR2A+/-) cancer cells. The treatment of cells at normal pH mimics (to some extent) the interactions of the agent with normal cells, taking into account that cancer cells, as opposed to normal cells, have lower cell surface pH even in a medium with normal pH (28–30).

The detailed description of all protocols can be found in the Supplementary Information.

Results

NIRF pHLIP imaging of human bladders

Fluorescent pHLIP agents (pHLIP-ICG used in 26 patients and pHLIP-IR800 used in 2 patients) were investigated in 64 lesions in 28 resected bladders (Table 1). Among the lesions investigated, 58 were cancerous and 6 were non-cancerous (from previous treatments). Information about types and grades of the investigated lesions is provided in Table 1 and Supplementary Table S1.

After surgery, the organ remains viable for a short period of time, continuing metabolic functions until cellular capacities are expended. We used all specimens immediately after their extraction, and all imaging was completed within two hours post radical cystectomy. No prominent histopathological alteration in the bladder mucosa or wall was noticed. Both ICG and IR800 are NIRF dyes with similar spectral properties suited well for clinical imaging systems. The representative light and pHLIP-ICG NIRF images of malignant lesions including carcinoma *in-situ* (CIS) and high grade invasive (HGI) urothelial carcinomas are shown in Figure 2. The imaging quality was not affected by the time of incubation with agents or choice of fluorophore (images of malignant lesion using NIRF pHLIP-IR800 are shown in Supplementary Figure S1). NIRF image processing was performed to establish lesion margins (Figure 3).

During gross evaluation using WL, 81% of the lesions were identified, while 98% of the lesions were seen under NIRF imaging. One lesion (inside a narrow-necked diverticulum with restricted access) seen under WL was not identified by NIRF imaging. Ten lesions missed under WL included two HGI and eight CIS. Compared to WL, NIRF evaluation with pHLIP demonstrated significantly higher sensitivity (98% vs. 81%; $p = 0.006$) and equal specificity (100% vs. 100%) in detection of malignant lesions (Supplementary Table S2).

NIRF evaluation with pHLIP also identified 6 non-cancerous lesions that represented treatment-related effects, including mucosal necrosis, granulation tissue formation, submucosal fibrous scar or granulomatous inflammation, diverticula with concomitant treatment effect and nephrogenic adenoma (NA) with associated treatment effects (all cases of NA were confirmed using PAX8 immunostaining). Normal tissues were not labeled by fluorescent pHLIP. Twelve randomly chosen, normal looking areas lacking NIRF signals were selected from different specimens as controls and were submitted for histopathology. Fluorescence images showed that mucosal hemorrhage and cystitis cystica et glandularis regions were not labeled by pHLIP (Supplementary Figure S2).

As an exploratory analysis in one case, *ex-vivo* laparoscopic cystoscopy imaging was performed (Figure 4). pHLIP-ICG

TABLE 1 Demographic information, pathological stage and diagnosis, lesions seen by white light (WL) and near-infrared fluorescence (NIRF) imaging with pHLIP-ICG or pHLIP-IF800.

Case #	Sex/Age	Stage	Pathological Diagnosis	Grade	Lesion	WL	NIRF	Construct
1	M/63	pT3aN1	Invasive high grade urothelial carcinoma, CIS	HGI	1	+	+	pHLIP-ICG
2	F/84	ypT3bN0	Invasive high grade papillary urothelial carcinoma	HGI	2	+	+	pHLIP-ICG
			Invasive high grade urothelial carcinoma	HGI	3	+	+	
3	M/51	pT2aN1	Invasive high grade urothelial carcinoma (micropapillary features)	HGI	4	+	+	pHLIP-ICG
4	M/69	pT1N0	Non-invasive high grade papillary urothelial carcinoma	HGN	5	+	+	pHLIP-ICG
			Invasive high grade urothelial carcinoma, CIS	HGI	6	+	+	
5	M/65	pTisN0	CIS	CIS	7	+	+	pHLIP-ICG
			CIS	CIS	8	+	+	
6	M/61	pT1N0	Invasive high grade urothelial carcinoma	HGI	9	+	+	pHLIP-ICG
7	M/79	pT0N0	Dysplasia	DYS	10	–	+	pHLIP-ICG
			Treatment effect	-	11	–	+	
8	F/82	pT1N0	Non-invasive high grade urothelial carcinoma	HGN	12	+	+	pHLIP-ICG
			Invasive high grade urothelial carcinoma	HGI	13	+	–	
			CIS	CIS	14	–	+	
			CIS	CIS	15	–	+	
9	M/68	pTisN0	CIS	CIS	16	+	+	pHLIP-ICG
			CIS	CIS	17	–	+	
10	M/71	pTaN0	Non-invasive high grade urothelial carcinoma	HGN	18	+	+	pHLIP-ICG
			Non-invasive high grade urothelial carcinoma	HGN	19	+	+	
			CIS	CIS	20	–	+	
			CIS	CIS	21	–	+	
11	F/77	pTisN0	CIS with early invasion	CIS	22	+	+	pHLIP-ICG
			CIS with early invasion	CIS	23	–	+	
12	M/57	pT1bN0	Invasive high grade papillary urothelial carcinoma	HGI	24	+	+	pHLIP-ICG
			CIS with early invasion	CIS	25	+	+	
			Treatment effect	-	26	+	+	
13	M/72	pT3aN0	Invasive high grade urothelial carcinoma, CIS	HGI	27	+	+	pHLIP-ICG
			Diverticulum and treatment effect	-	28	+	–	
14	M/66	ypT3aN0	Invasive high grade urothelial carcinoma (neuroendocrine features)	HGI	29	+	+	pHLIP-ICG
15	M/70	ypTisN0	CIS	CIS	30	+	+	pHLIP-ICG
			Treatment effect	-	31	-	+	
16	M/62	pT1bN0Mx	Invasive high grade papillary urothelial carcinoma	HGI	32	+	+	pHLIP-ICG
			Invasive high grade papillary urothelial carcinoma	HGI	33	+	+	
			Invasive high grade papillary urothelial carcinoma	HGI	34	+	+	
17	M/42	ypT3aN0Mx	Invasive high grade urothelial carcinoma (squamous features)	HGI	35	+	+	pHLIP-ICG
18	F/62	ypT2aN1Mx	Treatment effect	-	36	+	+	pHLIP-ICG
			Invasive high grade papillary urothelial carcinoma, CIS	HGI	37	-	+	
			Invasive high grade papillary urothelial carcinoma, CIS	HGI	38	-	+	
19	F/64	ypT1aN0Mx	Invasive high grade papillary urothelial carcinoma	HGI	39	+	+	pHLIP-ICG
			Invasive high grade papillary urothelial carcinoma	HGI	40	+	+	
20	M/79	pTisN0Mx	CIS	CIS	41	+	+	pHLIP-ICG
			CIS	CIS	42	+	+	
			CIS	CIS	43	-	+	
			CIS	CIS	44	-	+	
21	M/58	pT2bN0Mx	Invasive high grade papillary urothelial carcinoma, CIS	HGI	45	+	+	pHLIP-ICG
			Invasive high grade papillary urothelial carcinoma, CIS	HGI	46	+	+	
			Invasive high grade papillary urothelial carcinoma, CIS	HGI	47	+	+	

(Continued)

TABLE 1 Continued

Case #	Sex/ Age	Stage	Pathological Diagnosis	Grade	Lesion	WL	NIRF	Construct
22	M/80	pT3aN0Mx	Invasive high grade urothelial carcinoma (squamous, sarcomatoid and small cell features)	HGI	48	+	+	pHLIP-IR800
23	M/42	pT3aN2Mx	Invasive high grade papillary urothelial carcinoma	HGI	49	+	+	pHLIP-IR800
			Invasive high grade papillary urothelial carcinoma	HGI	50	+	+	
			Invasive high grade papillary urothelial carcinoma	HGI	51	+	+	
24	M/57	ypT3bN2Mx	Invasive high grade urothelial carcinoma (sarcomatoid features)	HGI	52	+	+	pHLIP-ICG
			Invasive high grade urothelial carcinoma (sarcomatoid features)	HGI	53	+	+	
25	M/76	pT1aN0Mx	Invasive high grade papillary urothelial carcinoma (squamous features)	HGI	54	+	+	pHLIP-ICG
26	M/63	pT2N0Mx	Invasive high grade papillary urothelial carcinoma (squamous features)	HGI	55	+	+	pHLIP-ICG
			Invasive high grade papillary Urothelial carcinoma (squamous features)	HGI	56	+	+	
			Invasive high grade papillary urothelial carcinoma (squamous features)	HGI	57	+	+	
27	F/81	pT2aN0Mx	Invasive high grade urothelial carcinoma (sarcomatoid features), CIS	HGI	58	+	+	pHLIP-ICG
			Invasive high grade urothelial carcinoma (sarcomatoid features), CIS	HGI	59	+	+	
			Invasive high grade urothelial carcinoma (sarcomatoid features), CIS	HGI	60	+	+	
			Invasive high grade urothelial carcinoma (sarcomatoid features), CIS	HGI	61	+	+	
28	M/74	mpT2aN0Mx	Invasive high grade papillary urothelial carcinoma	HGI	62	+	+	pHLIP-ICG
			Invasive high grade papillary urothelial carcinoma	HGI	63	+	+	
			Treatment effect	-	64	+	+	

F is Female, M is Male. When applicable, HGI is high grade invasive, HGN is high grade noninvasive, CIS is carcinoma *in situ*, and DIS is dysplasia. Treatment effects do not receive a grade or stage. Detailed staging definitions can be found in AJCC Cancer Staging Manual 7th edition section on Urinary Bladder.

targeting of HGI urothelial carcinoma lesion was confirmed with cystoscopy using a laparoscope (Figure 4B), while the nonmalignant mucosal hemorrhage area was not labeled with the agent (Figure 4E).

For CIS and HGI urothelial carcinomas we analyzed the homogeneity of the pHLIP-ICG signal (Figure 5). The fluorescence signal within lesions varied from 30-40 a.u. to 110-120 a.u. from the tumor margin to the tumor center,
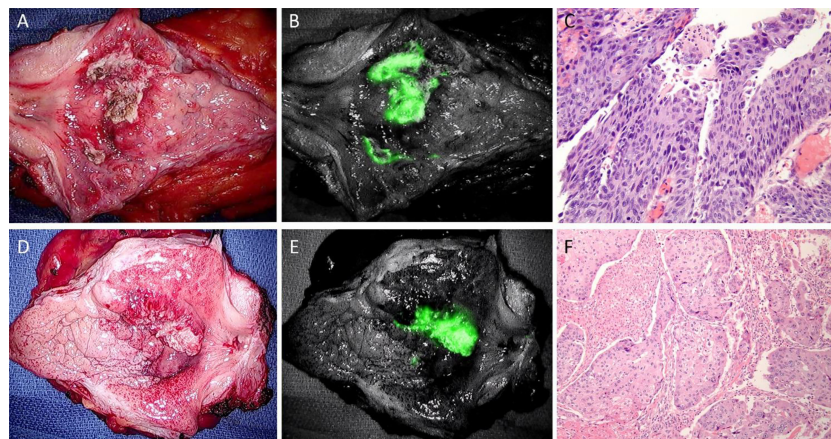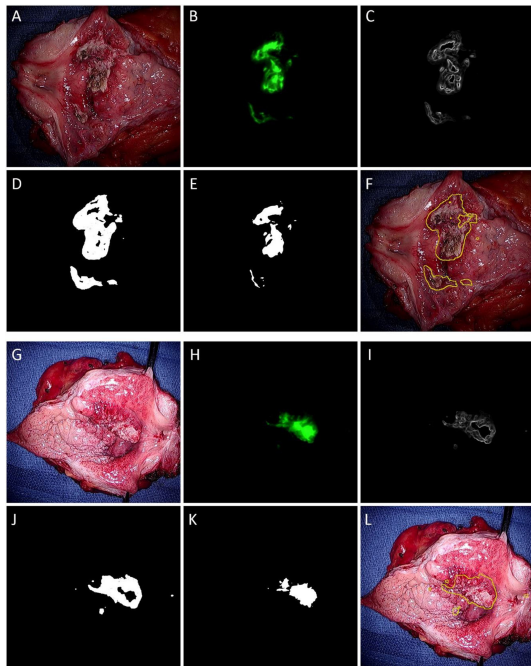

FIGURE 2
Imaging of malignant bladder lesions. **(A–C)**: case #20 with urothelial carcinoma *in-situ* (CIS) **(A)**, white light; **(B)**, pHLIP-ICG NIRF with white light; **(C)**, H&E 20x). **(D–F)**: case #17 with high grade invasive (HGI) urothelial carcinoma showing squamous differentiation **(D)**, white light; **(E)**, pHLIP-ICG NIRF with wight light; **(F)**, H&E 10x).
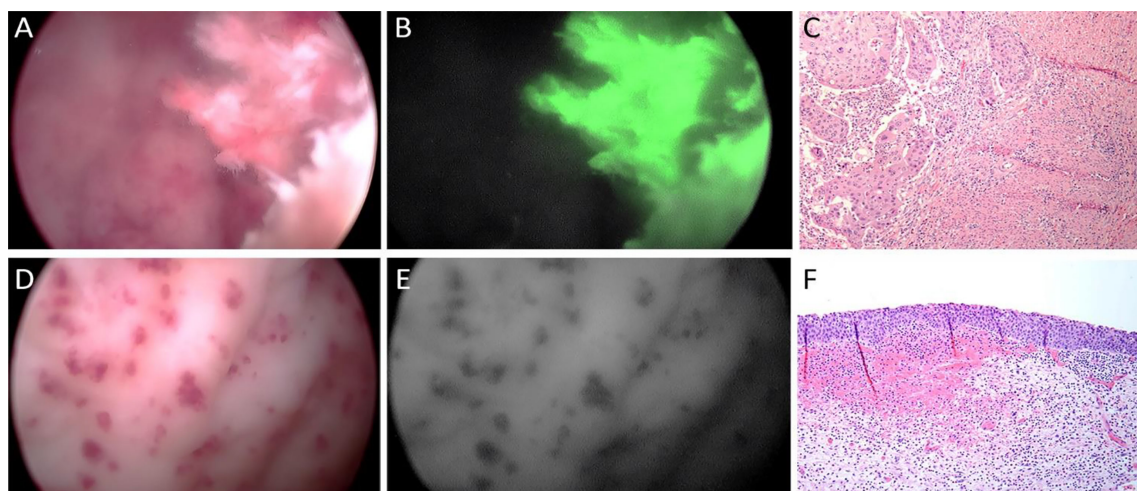
FIGURE 3
Margins of malignant lesions. **(A–F)**: case #20 with urothelial CIS and **(G–L)**: case #17 with HGI urothelial carcinoma. White light images **(A, G)**, pHLIP-ICG NIRF fluorescent images **(B, H)**, Sobel gradient field of B and H images **(C, I)**, binary mask of B and H images **(D, J)**, binary mask of C and I **(E, K)**, and white light images with fluorescent signal outline indicating tumor margins **(F, L)** are shown.

respectively, to confirm that the entire lesion is targeted by the pHLIP agent, which is important for both imaging and therapy.

Inhibition of urothelial cancer cell proliferation by pHLIP-amanitin

Having shown that pHLIP targets malignant lesions in bladders, we sought to pave the way for targeted delivery of therapeutic agents. We tested amanitin delivery as a possible therapy for the treatment of superficial malignant bladder lesions by intravesical instillation. Amanitin was linked to pHLIP *via* a cleavable S-S bond (pHLIP-Am) aiming to release amanitin in the cytoplasm of bladder cancer cells to induce cell cycle arrest and death. Amanitin, a polar, ~ 1 kDa cyclic peptide, has advantages as a cytotoxic agent for use with pHLIP as it has low cell membrane permeability, thus it will not enter cells by itself, and it has enhanced potency for cancer cells with 17p loss, which involves deletion of the tumor suppressor TP53 and POLR2A. This deletion often found in urothelial tumors.

As a test of pH-dependent delivery and mutant sensitivity, we studied pHLIP-Am inhibition of the proliferation of human breast cancer MDA-MB-231 WT cells (POLR2A+/+) and isogenic (POLR2A+/-) cells. Both WT and isogenic cell lines were treated with pHLIP-Am for 2 hrs in medium at pH 7.4 and 6.0, and for different time periods ranging from 0.5 to 2 hrs at pH 6.0 (Figure 6 and Table 2). The cytotoxicity of pHLIP-Am on isogenic cells compared to treatment of WT cells increased with incubation time at pH 6.0. The strongest cytotoxic effect and the largest difference (3-4x) between POLR2A+/- and POLR2A+/+

FIGURE 4
Ex-vivo laparoscopic cystoscopy. Case #17 with high grade invasive urothelial carcinoma white light **(A)**, pHLIP-ICG NIRF with white light **(B)**, and H&E 10x **(C)** images; and nonmalignant, signal free, control area showing mucosal hemorrhage white light **(D)**, pHLIP-ICG NIRF with white light **(E)**, and H&E 10x **(F)** images.
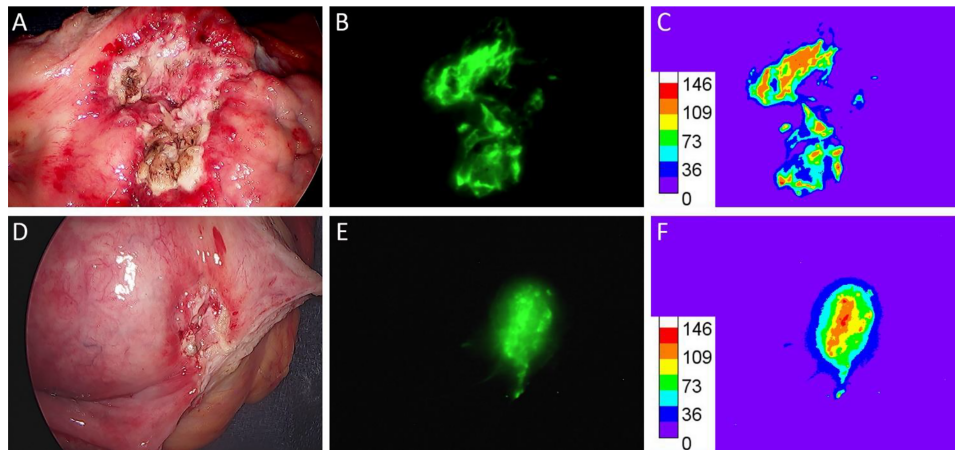
FIGURE 5
Intensity of within malignant lesions. Case #20 with urothelial carcinoma *in-situ* **(A−C)** and case #27 D-F with high grade invasive urothelial carcinoma with sarcomatoid features; white light images **(A, D)**; pHLIP-ICG NIRF images **(B, E)**; rainbow presentation of pHLIP-ICG NIRF images **(C, F)**.
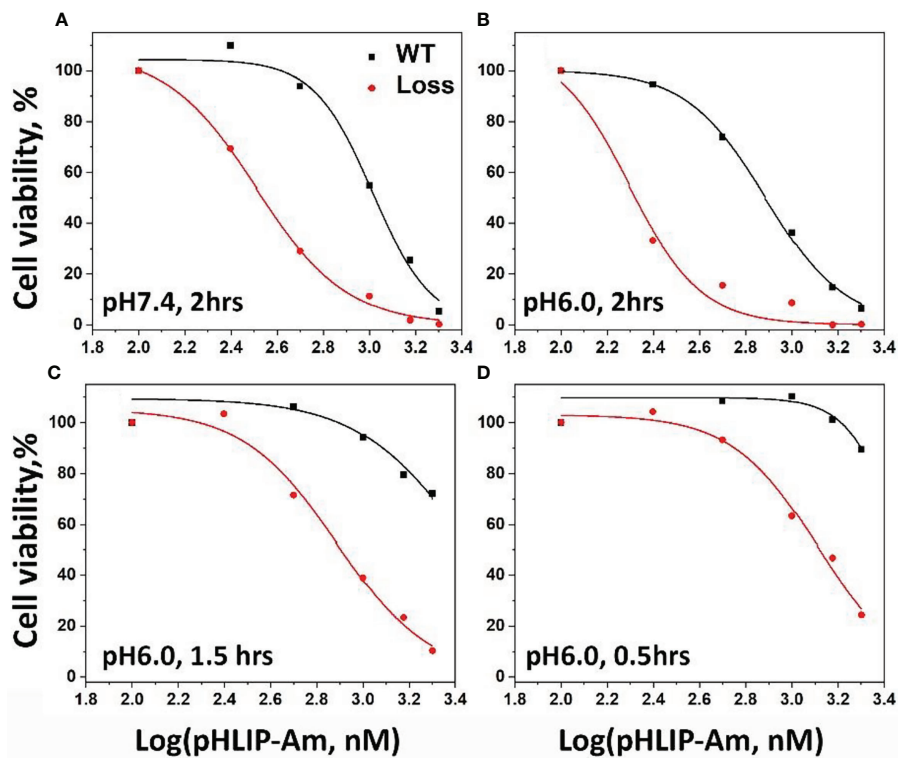
FIGURE 6
Viability of MDA-MB-231 cancer cells WT (POLR2A+/-) and isogenic (POLR2A+/-) after treatment with pHLIP-Am. Normalized WT and isogenic cell viability data, when cells were treated with different concentrations of pHLIP-Am at pH 7.4 for 2 hrs **(A)** and at pH 6.0 for different time periods **(B−D)**. The data were fitted by dose-response functions (curves) to calculate the EC_{50} values presented in Table 2.

TABLE 2   EC50 values were calculated for MDA-MB-231 WT (POLR2A+/+) and isogenic (POLR2A+/-) cell lines treated with pHLIP-Am at different conditions (cell viability data are shown on Figure 6).

Treatment conditions	EC50 (nM)WT cell line	EC50 (nM)Isogenic cell line	Fold difference
pHLIP-Am, pH7.4, 2.0 hrs	1031.1 ± 62.7	325.6 ± 18.6	3.2
pHLIP-Am, pH6.0, 2.0 hrs	770.6 ± 22.9	198.4 ± 26.1	3.9
pHLIP-Am, pH6.0, 1.5 hrs	2705.7 ± 706.4	772.5 ± 78.8	3.5
pHLIP-Am, pH6.0, 0.5 hrs	2834.9 ± 1183.1	1284.4 ± 75.2	2.2

The fold difference is the ratio of EC50 for WT to EC50 for isogenic cells.

cells were detected when pHLIP-Am was exposed to cells for 2 hrs at pH 6.0.

Inhibition of urothelial cancer cell proliferation by pHLIP-amanitin

Next, a range of well-characterized urothelial cancer cells of different grades were investigated, including squamous cell carcinoma, SCaBER, and transitional cell carcinomas, such as: UMUC3, SW780, RT4 - grade 1; 5637 - grade 2; J82, T24, HT-1376 - grade 3; TCCSUP, HT-1197 - grade 4. Urothelial cancer cells were treated with different concentrations of pHLIP-Am for 2 hrs at pH7.4 and 6.0. pH-Dependent bladder cancer cell death was observed as result of 2 hrs of treatment (Figure 7). In a control experiment, selected cell lines were treated with pHLIP and amanitin alone with no significant cytotoxic effect observed (Supplementary Figure S3).

The EC50 values (presented in Table 3) varied over a range from 28 nM to 430 nM, when cells were treated with the agent at pH6.0, and EC50 values varied from 211 nM to 2027 nM, when cells were treated with the agent at pH7.4. The efficacy of treatment or therapeutic index at low pH compared to normal pH ranged from 4 to 11 times for different bladder cancer cell lines.

We also investigated further pHLIP-Am cytotoxic effect in a wider range of pHs on the selected urothelial cancer cell lines of grade I (SW780) and grade II (5637). Cells were exposed to pHLIP-amanitin agent for 30 min at pHs 7.4, 6.0 and 5.0. The progressive increase of cytotoxicity was observed with decrease of pH of treatment (Supplementary Figure S4).

Discussion

We employed pHLIP technology for targeting of imaging and therapeutic cytotoxic agents to acidic urothelial carcinomas. It is well-established that cancer cells alter their metabolism to support their rapid proliferation and dissemination during tumor development and progression. Such an aberrant metabolism manifests itself in high rates of aerobic (Krebs cycle) and anaerobic (Warburg effect) glucose consumption and an overexpression of cell surface carbonic anhydrases that catalyze the transformation of carbon dioxide and water into carbonic acid (31–33). As a result of both anaerobic and aerobic glycolysis, and the overexpression of carbonic anhydrases, cancer cells exhibit elevated acidity in the vicinity of their plasma membranes (28–30). It has been shown in genetically engineered bladder cancer mouse models and human bladder cancers that overexpression of pyruvate kinase M2 promotes tumorigenesis by facilitating the Warburg effect and enhancing the activities of oncoproteins (34), and, thus, promoting acidification at the surface of urothelial cancer cells.

Fluorescent and narrow band endoscopic imaging improves the detection of malignant and premalignant urothelial carcinoma lesions compared to WL cystoscopy (35–40). Narrow band imaging in enhanced endoscopy allows from 34% to 100% sensitivity in the diagnosis of urothelial carcinoma (40). Similarly, compared to WL cystoscopy, blue light (BL) cystoscopy has been reported to provide up to a 24% improvement in the detection of papillary bladder tumors and up to a 43% improvement in the detection of carcinoma in situ (39). BL cystoscopy requires intravesical instillation and incubation of hexaminolevulinate for one hour, and the fluorescent signal fades within the next hour, narrowing the imaging time window (41). Additionally, BL cystoscopy with hexaminolevulinate is known to enhance some of the adverse effects associated with bladder cystoscopy and TURBT such as hematuria, dysuria, and bladder spasms (38, 42).

We have shown that fluorescent pHLIP-ICG targets urothelial carcinoma in ex-vivo human bladder specimens with excellent 98% sensitivity and 100%, specificity. Fluorescent pHLIP-ICG stains neoplastic cells after intravesical incubation, without targeting normal tissues. Histopathology of the unstained control areas revealed variable morphological features including cystitis cystica et glandularis and inflammation, indicating that pHLIP has low sensitivity to inflammation. Low-grade inflammation may be less acidic compared to cancer and therefore not targeted by pHLIP-ICG. Low sensitivity to inflammation may open an opportunity for the treatment of patients on hormonal therapies including 5-alpha reductase or androgen deprivation therapy (ADT), which
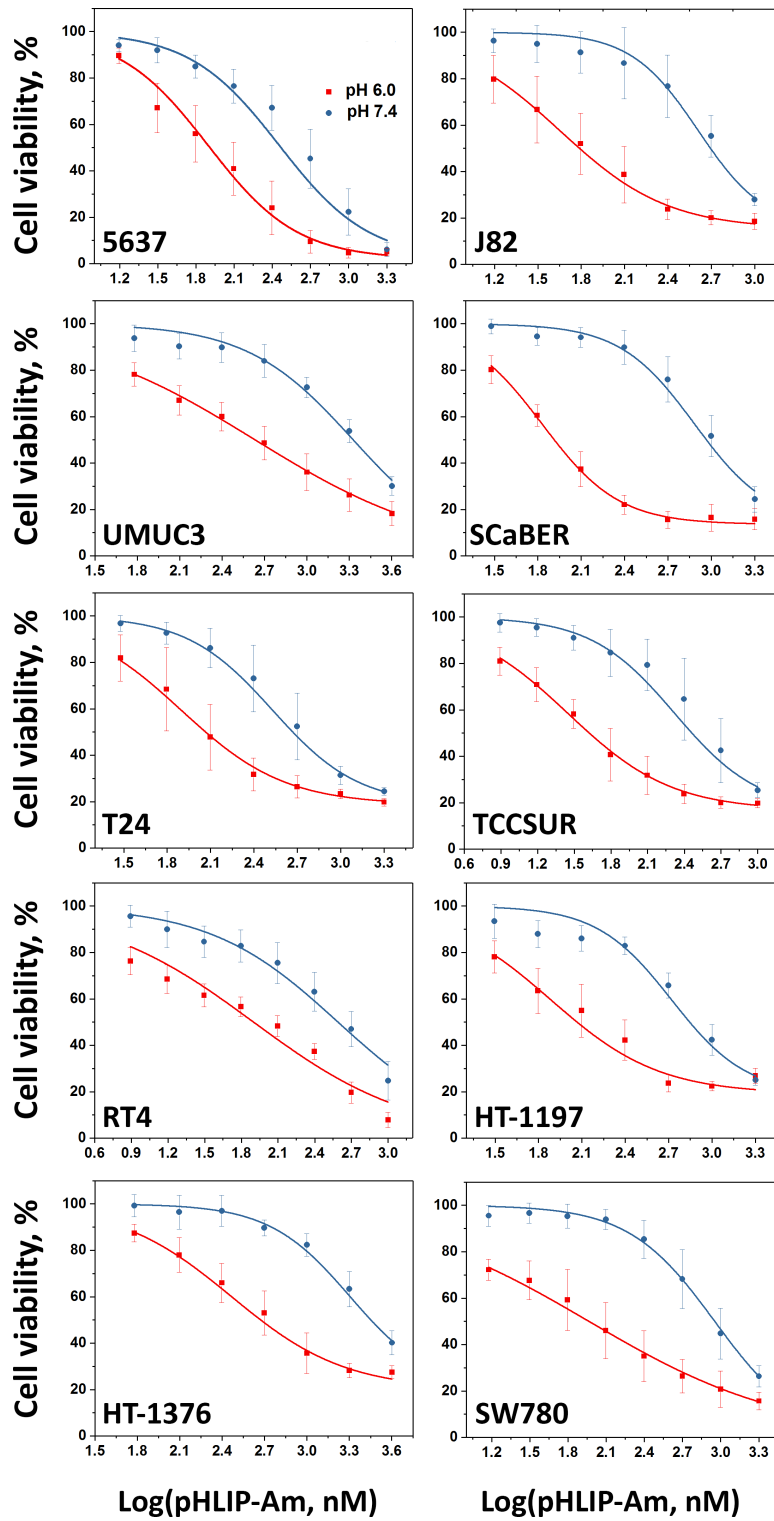
FIGURE 7

Urothelial cancer cells viability after treatment with pHLIP-Am. Normalized urothelial cancer cell viability data obtained when cells were treated with pHLIP-Am at pH 7.4 and 6.0 for 2 hrs. The data were fitted by dose-response functions (curves) to calculate the EC_{50} values presented in Table 3.

TABLE 3 EC50 values were calculated for each urothelial cancer cell type treated with pHLIP-Am at physiological (pH7.4) and low (pH6.0) pHs for 2 hrs (cell viability data are shown on Figure 7).

Cells	EC50 (nM) pH6.0	EC50 (nM) pH7.4	TI
5637 cells	78.5 ± 13.9	284.7 ± 41.6	3.6
J82 cells	45.1 ± 6.9	408.6 ± 40.0	9.1
UMUC3	429.8 ± 204.6	2128.8 ± 525.5	5.0
SCaBER	67.7 ± 4.7	768.2 ± 70.3	11.3
T24	79.3 ± 8.0	339.5 ± 22.2	4.3
TCCSUR	28.3 ± 2.7	211.1 ± 22.1	7.5
RT4	79.5 ± 10.8	390.0 ± 92.5	4.9
HT-1197	77.1 ± 22.2	527.4 ± 80.8	6.8
HT-1376	293.9 ± 47.2	2027.3 ±182.9	6.9
SW780	92.2 ± 31.9	900.2 ± 138.9	9.8

The therapeutic index (TI) is the ratio of EC50 at pH7.4 to EC50 at pH6.0.

reduce levels of male hormones and their immuno-suppressive signals (43, 44). The fluorescent pHLIP allowed identification of invasive and non-invasive carcinomas with different architectures (flat, solid, or papillary), grades (high or low), and subtypes (squamous, micropapillary, sarcomatoid and neuroendocrine carcinomas). The fluorescent pHLIP-ICG effectively identified urothelial CIS and dysplasia – non-invasive lesions which may be difficult to detect and treat using traditional white light techniques.

pHLIP-ICG has been translated to clinical trials at the Memorial Sloan Kettering Cancer Center, where a Phase I/IIa clinical trial (NCT05130801) has been initiated for fluorescence-guided surgery in breast cancer patients undergoing breast-conserving surgery. In phase I the patients receive pHLIP-ICG (a bolus IV injection on the day before surgery), and upon surgery the next day NIRF imaging using a Stryker Spy device is used to examine tumor tissue and margins. Several escalating doses of pHLIP-ICG will be tested in phase I, and safety assessments will be performed. The study performed with the lowest dose is completed and the data indicate tumor targeting and safety. After phase I is complete, pHLIP-ICG can be used in clinical trials for NIRF imaging in the diagnosis and treatment on other tumor indications, including urological tumors. For bladder cases, pHLIP-ICG could be administrated intravenously on the day before the procedure (NIRF cystoscopy or TURBT), or pHLIP-ICG could be administered to the bladder by intravesical instillation (for 15-30 min) before the procedure. The imaging window is expected to be wide: up to 24 hours after agent administration.

Specific targeting of malignant urothelial lesions by pHLIP peptides opens not only the possibility of improving imaging and resection of these lesions, but also supports the idea of treatments by pHLIP-targeted delivery of cytotoxic agents to bladder cancer cells. Therapeutic agents are administered systemically, for treatment of metastatic disease, or *via* intravesical instillation for treatment of superficial NMIBC.

We tested a highly toxic agent, amanitin, for targeted delivery with pHLIP for potential intravesical treatment of bladder cancers. Alpha-amanitin is a highly selective allosteric inhibitor of eukaryotic polymerase II (Pol II), which induces the degradation of Pol II resulting in cell death. Amanitin is one of the deadliest toxins known, exhibiting toxicity against both dividing and quiescent cells, which has made it an attractive payload for antibody drug conjugates (45–48). Amanitin is a polar molecule and exhibits limited permeability across cell membranes by itself, except in liver cells, which have a special transporting system for the uptake of small cyclic molecules like phallo- and amanita toxins (49). Recent success was achieved with targeted delivery of amanitin by Her2 antibody (50), and the agent entered clinical trials. Also, urothelial cancers are expected to be more sensitive to α-amanitin, which inhibits RNA Pol II encoded by POLR2A, since urothelial cancers frequently exhibit heterozygous loss of chromosome 17p (51–53), associated with deletion of the tumor suppressor TP53 and POLR2A (50, 54).

We have demonstrated that pHLIP-amanitin cytotoxic activity is 3-4x higher in cancer cells with 17p loss compared to WT when cells are treated for 2 hrs at pH 6.0. Our experiments on cultured urothelial cancer cells of different grades ranging from 1 to 4, when cells were exposed to pHLIP-amanitin for 2 hrs, mimic the conditions that might be used for intravesical treatment of superficial BC in humans. Grade is a good indicator for NMIBC progression and mortality, because patients with high-grade tumors progress with similar frequency regardless of whether they were invasive or noninvasive (55, 56). The maximum concentration of pHLIP-amanitin was 2-4 μM (in different experiments), which is comparable to the pHLIP concentration used in the imaging study, where a solution containing 4 μM of fluorescent pHLIP was sufficient for targeting of malignant lesions. It is expected that systemic exposure, and thus the systemic toxicity of pHLIP-amanitin could be lower compared to small molecule drugs

applied *via* intravesical instillation, since the adsorption of pHLIP-amanitin (molecular weight ~5 kDa) is expected to be significantly lower compared to drugs that are 10x smaller. We also note that the volume and pH of urine can be controlled and kept at pH 7.4 by supplying bicarbonate drinks and antidiuretics several days prior to and after intravesical instillation: alkalization of urine is a practice adopted in the clinics and widely used (57, 58). Thus, even if some amount of urine is drained into bladder during a 1 hr intravesical instillation period, the drained urine will not alter the pH of the buffered solution used for instillation to avoid targeting of all cells in the bladder. The results we report here are encouraging, and the therapeutic efficacy, potential system exposure and overall toxicity of pHLIP-based agents are now under study in transgenic bladder cancer mouse models.

A therapeutic trial is in progress using a different therapeutic conjugate, pHLIP-exatecan (CBX-12) (59), where exatecan is a cytotoxic inhibitor of Topoisomerase I. The pHLIP construct was systemically administrated to patients with advanced metastatic cancer in phase I/II clinical trials (NCT04902872) with very promising initial results. Systemic administration of an agent leads to its exposure to a highly dynamic system with fast blood circulation and clearance. However, intravesical instillation for bladder cancer would result in a relatively stationary exposure of an agent to the entire bladder. In the latter case, the use of a polar, cell-impermeable therapeutic payload such as an amanitin, as opposed to a more hydrophobic drug like exatecan, is preferable since it will reduce adsorption and potential uptake of pHLIP-amanitin by normal cells. Also, if any amanitin is released in the lumen, it would be unlikely to cause serious toxicity, since amanitin is cell-impermeable.

The pHLIP technology may present several opportunities for improved management of urothelial cancer. Imaging and treatment of superficial bladder cancers might be performed *via* intravesical instillation of pHLIP-ICG (for diagnosis and TURBT) or pHLIP-amanitin (to kill tumor cells). Furthermore, the pHLIP-Zr PET imaging agent, therapeutic pHLIP-exatecan and other pHLIP-based therapeutic agents that are currently under development, might be used for imaging and treatment of metastatic disease *via* systemic administration of the agents.

Data availability statement

The raw data supporting the conclusions of this article will be made available by the authors, without undue reservation.

Ethics statement

The studies involving human participants were reviewed and approved by Institutional Review Board of Lifespan and The Miriam Hospital. The patients/participants provided their written informed consent to participate in this study.

Author contributions

Funding

Acknowledgments

Conflict of interest

DE, OA and YR are founders of pHLIP, Inc., and they have shares in the company. pHLIP, Inc did not provide funding for the research. XL has a U.S. patent (no. 10563204) on "Methods of treating cancer harboring hemizygous loss of TP53" licensed to Heidelberg Pharma AG.

The remaining authors declare that the research was conducted in the absence of any commercial or financial relationships that could be construed as a potential conflict of interest.

Publisher's note

Supplementary material

The Supplementary Material for this article can be found online at: https://www.frontiersin.org/articles/10.3389/fruro.2022.868919/full#supplementary-material

SUPPLEMENTARY TABLE 1
Summary of malignant lesions (*n*=58). All data reported as *n* (%).

SUPPLEMENTARY TABLE 2
Results of Sensitivity and Specificity tests for malignant lesions.

SUPPLEMENTARY FIGURE 1
Imaging of malignant bladder lesion with pHLIP-IR800. Caase #22 with high grade invasive (HGI) small cell carcinoma (**A**, white light; H, pHLIP-IR800 NIRF with white light; **B**, H&E 10x).

SUPPLEMENTARY FIGURE 2
Randomly chosen negative control areas. (**A–C**) Case #17 showing mucosal hemorrhage and cystitis cystica et glandularis (**A**, white light; **B**, pHLIP NIRF; **C**, H&E 10x). (**D–F**) Case #22 (**D**, white light; **E**, pHLIP NIRF; **F**, H&E 10x). (**G–I**) Case #27 (**G**, white light; **H**, pHLIP NIRF; **I**, H&E 10x).

SUPPLEMENTARY FIGURE 3
Urothelial cancer cells viability after treatment with pHLIP or amanitin. Normalized urothelial cancer cell viability data obtained when cells were treated with pHLIP or amanitin at pH 7.4 and 6.0 for 2 hrs.

SUPPLEMENTARY FIGURE 4
Urothelial cancer cells viability after treatment with pHLIP-Am at different pHs. Normalized urothelial cancer cell viability data obtained when cells were treated with pHLIP-Am at pH 7.4, 6.0 or 5.0 for 30 min in 10 mM phosphate buffer containing 150 mM NaCl, 1 mM $CaCl_2$, 0.5 mM $MgCl_2$.

References

1. Siegel RL, Miller KD, Jemal A. Cancer statistics, 2019. *CA Cancer J Clin* (2019) 69:7–34. doi: 10.3322/caac.21551

2. Woldu SL, Bagrodia A, Lotan Y. Guideline of guidelines: non-muscle-invasive bladder cancer. *BJU Int* (2017) 119:371–80. doi: 10.1111/bju.13760

3. Sanguedolce F, Cormio A, Bufo P, Carrieri G, Cormio L. Molecular markers in bladder cancer: Novel research frontiers. *Crit Rev Clin Lab Sci* (2015) 52:242–55. doi: 10.3109/10408363.2015.1033610

4. Nicolazzo C, Busetto GM, Del Giudice F, Sperduti I, Giannarelli D, Gradilone A, et al. The long-term prognostic value of survivin expressing circulating tumor cells in patients with high-risk non-muscle invasive bladder cancer (NMIBC). *J Cancer Res Clin Oncol* (2017) 143:1971–6. doi: 10.1007/s00432-017-2449-8

5. Laukhtina E, Abufaraj M, Al-Ani A, Ali MR, Mori K, Moschini M, et al. Intravesical therapy in patients with intermediate-risk nonmuscle-invasive bladder cancer: A systematic review and network meta-analysis of disease recurrence. *Eur Urol Focus* (2021) 8(2):447–56. doi: 10.1016/j.euf.2021.03.016

6. Joice GA, Bivalacqua TJ, Kates M. Optimizing pharmacokinetics of intravesical chemotherapy for bladder cancer. *Nat Rev Urol* (2019) 16:599–612. doi: 10.1038/s41585-019-0220-4

7. Wyatt LC, Lewis JS, Andreev OA, Reshetnyak YK, Engelman DM. Applications of pHLIP technology for cancer imaging and therapy. *Trends Biotechnol* (2017) 35:653–64. doi: 10.1016/j.tibtech.2017.03.014

8. Reshetnyak YK, Moshnikova A, Andreev OA, Engelman DM. Targeting acidic diseased tissues by pH-triggered membrane-associated peptide folding. *Front Bioeng Biotechnol* (2020) 8:335. doi: 10.3389/fbioe.2020.00335

9. Reshetnyak YK, Segala M, Andreev OA, Engelman DM. A monomeric membrane peptide that lives in three worlds: in solution, attached to, and inserted across lipid bilayers. *Biophys J* (2007) 93:2363–72. doi: 10.1529/biophysj.107.109967

10. Andreev OA, Karabadzhak AG, Weerakkody D, Andreev GO, Engelman DM, Reshetnyak YK. pH (low) insertion peptide (pHLIP) inserts across a lipid bilayer as a helix and exits by a different path. *Proc Natl Acad Sci U.S.A.* (2010) 107:4081–6. doi: 10.1073/pnas.0914330107

11. Hunt JF, Rath P, Rothschild KJ, Engelman DM. Spontaneous, pH-dependent membrane insertion of a transbilayer alpha-helix. *Biochemistry* (1997) 36:15177–92. doi: 10.1021/bi970147b

12. Golijanin J, Amin A, Moshnikova A, Brito JM, Tran TY, Adochite RC, et al. Targeted imaging of urothelium carcinoma in human bladders by an ICG pHLIP peptide ex vivo. *Proc Natl Acad Sci USA* (2016) 113(42):11829–34. doi: 10.1073/pnas.1610472113

13. Brito J, Golijanin B, Kott O, Moshnikova A, Mueller-Leonhard C, Gershman B, et al. Ex-vivo imaging of upper tract urothelial carcinoma using novel pH low insertion peptide (Variant 3), a molecular imaging probe. *Urology* (2020) 139:134–40. doi: 10.1016/j.urology.2019.01.008

14. Moshnikova A, Moshnikova V, Andreev OA, Reshetnyak YK. Antiproliferative effect of pHLIP-amanitin. *Biochemistry* (2013) 52:1171–8. doi: 10.1021/bi301647y

15. Weerakkody D, Moshnikova A, El-Sayed NS, Adochite RC, Slaybaugh G, Golijanin J, et al. Novel pH-sensitive cyclic peptides. *Sci Rep* (2016) 6:31322. doi: 10.1038/srep31322

16. Wyatt LC, Moshnikova A, Crawford T, Engelman DM, Andreev OA, Reshetnyak YK. Peptides of pHLIP family for targeted intracellular and extracellular delivery of cargo molecules to tumors. *Proc Natl Acad Sci U.S.A.* (2018) 115:E2811–8. doi: 10.1073/pnas.1715350115

17. An M, Wijesinghe D, Andreev OA, Reshetnyak YK, Engelman DM. pH-(low)-insertion-peptide (pHLIP) translocation of membrane impermeable phalloidin toxin inhibits cancer cell proliferation. *Proc Natl Acad Sci U.S.A.* (2010) 107:20246–50. doi: 10.1073/pnas.1014403107

18. Wijesinghe D, Engelman DM, Andreev OA, Reshetnyak YK. Tuning a polar molecule for selective cytoplasmic delivery by a pH (Low) insertion peptide. *Biochemistry* (2011) 50:10215–22. doi: 10.1021/bi2009773

19. O'Toole C, Price ZH, Ohnuki Y, Unsgaard B. Ultrastructure, karyology and immunology of a cell line originated from a human transitional-cell carcinoma. *Br J Cancer* (1978) 38:64–76. doi: 10.1038/bjc.1978.164

20. Grossman HB, Wedemeyer G, Ren L, Wilson GN, Cox B. Improved growth of human urothelial carcinoma cell cultures. *J Urol* (1986) 136:953–9. doi: 10.1016/S0022-5347(17)45139-1

21. O'Toole C, Nayak S, Price Z, Gilbert WH, Waisman J. A cell line (SCABER) derived from squamous cell carcinoma of the human urinary bladder. *Int J Cancer* (1976) 17:707–14. doi: 10.1002/ijc.2910170604

22. Bubenik J, Baresova M, Viklicky V, Jakoubkova J, Sainerova H, Donner J. Established cell line of urinary bladder carcinoma (T24) containing tumour-specific antigen. *Int J Cancer* (1973) 11:765–73. doi: 10.1002/ijc.2910110327

23. Nayak SK, O'Toole C, Price ZH. A cell line from an anaplastic transitional cell carcinoma of human urinary bladder. *Br J Cancer* (1977) 35:142–51. doi: 10.1038/bjc.1977.21

24. Rigby CC, Franks LM. A human tissue culture cell line from a transitional cell tumour of the urinary bladder: growth, chromosome pattern and ultrastructure. *Br J Cancer* (1970) 24:746–54. doi: 10.1038/bjc.1970.89

25. Rasheed S, Gardner MB, Rongey RW, Nelson-Rees WA, Arnstein P. Human bladder carcinoma: characterization of two new tumor cell lines and search for tumor viruses. *J Natl Cancer Inst* (1977) 58:881–90. doi: 10.1093/jnci/58.4.881

26. Fogh J. Cultivation, characterization, and identification of human tumor cells with emphasis on kidney, testis, and bladder tumors. *Natl Cancer Inst Monogr* (1978) 49:5–9.

27. Williams RD. Human urologic cancer cell lines. *Invest Urol* (1980) 17:359–63.

28. Anderson M, Moshnikova A, Engelman DM, Reshetnyak YK, Andreev OA. Probe for the measurement of cell surface pH *in vivo* and ex vivo. *Proc Natl Acad Sci U.S.A.* (2016) 113:8177–81. doi: 10.1073/pnas.1608247113

29. Wei D, Engelman DM, Reshetnyak YK, Andreev OA. Mapping pH at cancer cell surfaces. *Mol Imaging Biol* (2019) 21:1020–5. doi: 10.1007/s11307-019-01335-4

30. Podder A, Joseph MM, Biswas S, Samanta S, Maiti KK, Bhuniya S. Amphiphilic fluorescent probe self-encored in plasma to detect pH fluctuations

in cancer cell membranes. *Chem Commun (Camb)* (2021) 57:607–10. doi: 10.1039/D0CC06694J

31. Wykoff CC, Beasley NJ, Watson PH, Turner KJ, Pastorek J, Sibtain A, et al. Hypoxia-inducible expression of tumor-associated carbonic anhydrases. *Cancer Res* (2000) 60:7075–83.

32. Potter CP, Harris AL. Diagnostic, prognostic and therapeutic implications of carbonic anhydrases in cancer. *Br J Cancer* (2003) 89:2–7. doi: 10.1038/sj.bjc.6600936

33. Swietach P, Patiar S, Supuran CT, Harris AL, Vaughan-Jones RD. The role of carbonic anhydrase 9 in regulating extracellular and intracellular ph in three-dimensional tumor cell growths. *J Biol Chem* (2009) 284:20299–310. doi: 10.1074/jbc.M109.006478

34. Xia Y, Wang X, Liu Y, Shapiro E, Lepor H, Tang MS, et al. PKM2 is essential for bladder cancer growth and maintenance. *Cancer Res* (2022) 82:571–85. doi: 10.1158/0008-5472.CAN-21-0403

35. Hermann GG, Mogensen K, Carlsson S, Marcussen N, Duun S. Fluorescence-guided transurethral resection of bladder tumours reduces bladder tumour recurrence due to less residual tumour tissue in Ta/T1 patients: a randomized two-centre study. *BJU Int* (2011) 108:E297–303. doi: 10.1111/j.1464-410X.2011.10090.x

36. Herr HW. Narrow-band imaging cystoscopy to evaluate the response to bacille calmette-guerin therapy: preliminary results. *BJU Int* (2010) 105:314–6. doi: 10.1111/j.1464-410X.2009.08788.x

37. Naselli A, Introini C, Timossi L, Spina B, Fontana V, Pezzi R, et al. A randomized prospective trial to assess the impact of transurethral resection in narrow band imaging modality on non-muscle-invasive bladder cancer recurrence. *Eur Urol* (2012) 61:908–13. doi: 10.1016/j.eururo.2012.01.018

38. Daneshmand S, Bazargani ST, Bivalacqua TJ, Holzbeierlein JM, Willard B, Taylor JM, et al. Blue light cystoscopy for the diagnosis of bladder cancer: Results from the US prospective multicenter registry. *Urol Oncol* (2018) 36:361.e1–6. doi: 10.1016/j.urolonc.2018.04.013

39. Burger M, Grossman HB, Droller M, Schmidbauer J, Hermann G, Drăgoescu O, et al. Photodynamic diagnosis of non–muscle-invasive bladder cancer with hexaminolevulinate cystoscopy: A meta-analysis of detection and recurrence based on raw data. *Eur Urol* (2013) 64:846–54. doi: 10.1016/j.eururo.2013.03.059

40. Hsueh TY, Chiu AW. Narrow band imaging for bladder cancer. *Asian J Urol* (2016) 3:126–9. doi: 10.1016/j.ajur.2016.05.001

41. Zlatev DV, Altobelli E, Liao JC. Advances in imaging technologies in the evaluation of high-grade bladder cancer. *Urol Clin North Am* (2015) 42:147–57, vii. doi: 10.1016/j.ucl.2015.01.001

42. Yang LP. Hexaminolevulinate blue light cystoscopy: a review of its use in the diagnosis of bladder cancer. *Mol Diagn Ther* (2014) 18:105–16. doi: 10.1007/s40291-013-0068-x

43. Busetto GM, Giovannone R, Antonini G, Rossi A, Del Giudice F, Tricarico S, et al. Short-term pretreatment with a dual 5alpha-reductase inhibitor before bipolar transurethral resection of the prostate (B-TURP): evaluation of prostate vascularity and decreased surgical blood loss in large prostates. *BJU Int* (2015) 116:117–23. doi: 10.1111/bju.12917

44. Salciccia S, Del Giudice F, Gentile V, Mastroianni CM, Pasculli P, Di Lascio G, et al. Interplay between male testosterone levels and the risk for subsequent invasive respiratory assistance among COVID-19 patients at hospital admission. *Endocrine* (2020) 70:206–10. doi: 10.1007/s12020-020-02515-x

45. Vetter J. Toxins of amanita phalloides. *Toxicon* (1998) 36:13–24. doi: 10.1016/S0041-0101(97)00074-3

46. Nicolaou KC, Rigol S. The role of organic synthesis in the emergence and development of antibody-drug conjugates as targeted cancer therapies. *Angew Chem Int Ed Engl* (2019) 58:11206–41. doi: 10.1002/anie.201903498

47. Moldenhauer G, Salnikov AV, Luttgau S, Herr I, Anderl J, Faulstich H. Therapeutic potential of amanitin-conjugated anti-epithelial cell adhesion molecule monoclonal antibody against pancreatic carcinoma. *J Natl Cancer Inst* (2012) 104:622–34. doi: 10.1093/jnci/djs140

48. Davis MT, Preston JF3rd. A conjugate of alpha-amanitin and monoclonal immunoglobulin G to thy 1.2 antigen is selectively toxic to T lymphoma cells. *Science* (1981) 213:1385–8. doi: 10.1126/science.6115471

49. Munter K, Mayer D, Faulstich H. Characterization of a transporting system in rat hepatocytes. studies with competitive and non-competitive inhibitors of phalloidin transport. *Biochim Biophys Acta* (1986) 860:91–8. doi: 10.1016/0005-2736(86)90502-X

50. Li Y, Sun Y, Kulke M, Hechler T, van der Jeught K, Dong T, et al. Targeted immunotherapy for HER2-low breast cancer with 17p loss. *Sci Transl Med* (2021) 13(580). doi: 10.1126/scitranslmed.abc6894

51. Rivlin N, Brosh R, Oren M, Rotter V. Mutations in the p53 tumor suppressor gene: Important milestones at the various steps of tumorigenesis. *Genes Cancer* (2011) 2:466–74. doi: 10.1177/1947601911408889

52. Habuchi T, Ogawa O, Kakehi Y, Ogura K, Koshiba M, Sugiyama T, et al. Allelic loss of chromosome 17p in urothelial cancer: strong association with invasive phenotype. *J Urol* (1992) 148:1595–9. doi: 10.1016/S0022-5347(17)36977-X

53. Habuchi T, Ogawa O, Kakehi Y, Ogura K, Koshiba M, Hamazaki S, et al. Accumulated allelic losses in the development of invasive urothelial cancer. *Int J Cancer* (1993) 53:579–84. doi: 10.1002/ijc.2910530409

54. Liu Y, Zhang X, Han C, Wan G, Huang X, Ivan C, et al. TP53 loss creates therapeutic vulnerability in colorectal cancer. *Nature* (2015) 520:697–701. doi: 10.1038/nature14418

55. Knowles MA, Hurst CD. Molecular biology of bladder cancer: new insights into pathogenesis and clinical diversity. *Nat Rev Cancer* (2015) 15:25–41. doi: 10.1038/nrc3817

56. van Rhijn BW, Burger M, Lotan Y, Solsona E, Stief CG, Sylvester RJ, et al. Recurrence and progression of disease in non-muscle-invasive bladder cancer: from epidemiology to treatment strategy. *Eur Urol* (2009) 56:430–42. doi: 10.1016/j.eururo.2009.06.028

57. Krarup-Hansen A, Wassermann K, Rasmussen SN, Dalmark M. Pharmacokinetics of doxorubicin in man with induced acid or alkaline urine. *Acta Oncol* (1988) 27:25–30. doi: 10.3109/02841868809090314

58. Cliff AM, Heatherwick B, Scoble J, Parr NJ. The effect of fasting or desmopressin before treatment on the concentration of mitomycin c during intravesical administration. *BJU Int* (2000) 86:644–7. doi: 10.1046/j.1464-410x.2000.00869.x

59. Gayle S, Aiello R, Leelatian N, Beckta JM, Bechtold J, Bourassa P, et al. Tumor-selective, antigen-independent delivery of a pH sensitive peptide-topoisomerase inhibitor conjugate suppresses tumor growth without systemic toxicity. *NAR Cancer* (2021) 3:zcab021. doi: 10.1093/narcan/zcab021